

Céline, A., **Fréour, S.**, Jacquemin, F., Casari, P. (2013). Characterization and modeling of the moisture diffusion behaviour of natural fibres, *Journal of Applied Polymer Science*, **130**(1), 297-306.

Characterization and modeling of the moisture diffusion behaviour of natural fibres

Amandine Céline, Sylvain Fréour, Frédéric Jacquemin, Pascal Casari

Institut de Recherche en Génie Civil et Mécanique (UMR CNRS 6183),

LUNAM Université - Université de Nantes - Centrale Nantes

CRTT, 37 Boulevard de l'Université, BP 406, 44602 Saint-Nazaire cedex, France

Corresponding author: Amandine Céline

Telephone number: +33240172625

Fax number: +33240172618

E-mail address: amandine.celino@univ-nantes.fr

Abstract

Natural fibres have good properties to be used as reinforcement in composite materials. The main issue is their hydrophilic behaviour. So we propose here, to investigate the diffusion phenomenon in such fibres. First, a brief characterization of four kind of vegetal fibres (hemp, jute, flax and sisal) has been achieved. We show that all fibres have a similar composition and structure despite their different origin. Then, their moisture diffusive behaviour was investigated. The samples were submitted to hygro-thermal ageing either in total water immersion at room temperature or in an environmental chamber at 80 % relative humidity and 23°C. Various predictive models were used to simulate experimental curves. Results show that all fibres exhibit a similar diffusive behaviour in a same environment. In immersion specimens show anomalous absorption kinetics and Langmuir theory actually describes very well the diffusion kinetics in such conditions whereas the same fibres follow a Fickian diffusion when they are exposed to vapor during relative humidity ageing.

Keywords

natural fibres, durability, diffusion, Langmuir

1 Introduction

Since several years, with the growth of the environmental concern, bio-based materials have been more extensively studied for specific applications. In the field of composite materials, natural fibres are actually considered as a possible alternative to glass fibres for reinforcing polymeric matrix in automotive engineering, particularly [1-3]. They are light, abundant and renewable. Moreover, they exhibit higher specific mechanical properties than glass fibres because of their low density [4]. The main issue related to the use of plant fibres, is their hydrophilic behaviour due to free hydroxyl groups. Understanding the interactions between natural fibres and water is of great importance, due to the pronounced influence of moisture on their mechanical properties as well as on dimensional changes [5,6]. Therefore, the adhesion with hydrophobic matrix is not strong enough and the ageing of composite materials reinforced by plant fibers can lead to a premature degradation and the loss of their mechanical properties [7,8]. Many practical investigations have been achieved to modify the structure of natural fibres in order to reduce their hydrophilic characteristic [9-12]. However, few people have explored the diffusion phenomenon inside these fibres to understand the mechanism of moisture absorption [13,14]. Various physical models describing diffusion phenomenon inside polymers are available in literature. Among them, Fick's law is the most common model used [15,16]. However, some polymers present anomalous Fickian diffusion [17,18]. In these cases others models can be used as Langmuir theory [19] or a dual stage Fick law [20]. In the purpose of bio-based fibres, more recently, Kohler et al., used a mathematical equation to describe kinetics of water vapor sorption inside cellulosic fibres [21]. The numerical fitting proposed in the paper doesn't enable the identification of diffusion parameters nor the prediction of the moisture content spatial distribution along thickness as in classical models. Yet, this is of great importance to study the mechanical states inside materials in the transient state. As an example, reference [22] constitutes an interesting theoretical work where the authors determined the spatial distribution of moisture content inside cylindrical material and the resulting mechanical stresses by using both a Fickian and a hygroelastic model.

In the present work, we intend to use these classical diffusion models on four natural fibres diffusion kinetics. In a first time, a characterization of our fibres has been achieved. Fourier Transform InfraRed Spectroscopy (FTIR

spectroscopy) analysis allowed investigating the composition, X-ray diffraction enabled to quantify the crystallinity, while Scanning Electron Microscopy (SEM) was used to observe the surface morphology. Eventually, fibres densities were determined owing to pycnometry. In a second time, kinetics diffusion of the fibres was independently studied in vapor humidity and liquid water. Experimentally, the samples were submitted to hygro-thermal ageing, either through liquid water immersion at room temperature or in an environmental chamber at 80 % relative humidity and 23°C. Periodic gravimetric measurements were achieved on the specimens in order to study the weight gain as a function of the time. Numerical modeling was intended to identify the diffusive parameters of each fibre and provide an enhanced understanding of the mechanism of moisture absorption inside such bio-based constituents.

2 Materials and methods

2.1. Materials

Fibres studied are hemp, flax, jute and sisal. Among plant fibres these one present the best mechanical properties regarding glass fibres replacement for the purpose of reinforcing polymeric matrix (**Table 1**) [23,24]. Flax, hemp and jute are extracted from the stem of the plant whereas sisal is extracted from the leaf. As shown in **Figure 1**, plant fibres have a multi-scale structure. Thus, the diffusion of water is influencing by the fibre structure at different scales. In the unit fibre scale, the fibre exhibits a complex multi cell wall structure (**Figure 1-c**). This structure can in first approximation be assumed to behave similarly to its higher layer S2 which usually constitutes more than 80 % of the total diameter (**Figure 1-d**) [26]. Actually, this layer is assumed to be a composite material with an amorphous phase (matrix) reinforced by a rigid crystalline phase (cellulose microfibrils) [27]. At this scale, diffusion of water would take place in the amorphous region. Besides, these regions are mainly composed by hydrophilic polymers (hemicelluloses and lignin). In the bundle scale (**Figure 1-b**), diffusion is privileged trough the interface between fibres. This interface is called middle lamella. According to Morvan et al. [25] the middle lamella is principally composed by pectin where the carboxyl functions make easier the absorption of water by hydrogen bonding. The last structural factor influencing diffusion is the general porous structure of natural fibres. Water could be trapped inside pores.

In the following study, bundles of hemp, flax, jute and sisal fibres have been characterized.

fibre	Density (g/cm ³)	Specific stress (MPa.cm ³ /g)	Specific Young Modulus (GPa.cm ³ /g)
Jute	1.3-1.46	286-650	7-22
Flax	1.4-1.55	238-1000	34-76
Hemp	1.4-1.5	214-1264	24-50
E-Glass	2.55	941	29

Table 1. Mechanical properties of different fibres [23,24,28]

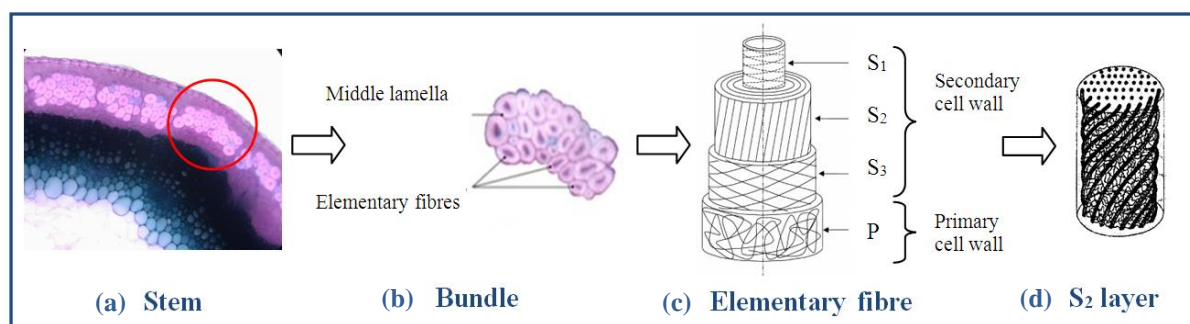


Fig.1 Multi-scale structure of the flax fibre [25,27]

2.2. Characterization

2.2.1. Fourier Transform InfraRed Spectroscopy

In order to compare their composition, Fourier Transform Infrared Spectroscopy (FTIR) was carried out on the four fibres in ambient conditions. Bundles were submitted to FTIR spectrometer using a Bruker Tensor 27 stage operating in ATR (Attenuated Total Reflectance) mode with a diamond crystal. Scanning was conducted in the frequency range 4000-400 cm⁻¹ with a 32 repetitious scan average for each sample and a resolution of 2cm⁻¹. No treatment have been achieved on the obtained spectra. As the molecule in the cellulose chain will vibrate differently in well ordered crystalline phases compared to less ordered phases it is possible to assign absorption band to

crystalline and amorphous region [29]. Then a crystallinity index could be evaluated. In this study, Total Crystallinity Index established by Nelson and O'Connor in the 60's [30] has been calculated using ratio between the absorption band at 1375 cm^{-1} characteristic of cellulose crystalline phase and the absorption band at 2900 cm^{-1} from the amorphous phase. These results will be compared to crystallinity indices obtained by Segal's method using X-ray analysis (section 2.2.2). It should be noted that this method gives only relative values, because the spectrum always contains contributions from both crystalline and amorphous regions.

2.2.2. X-ray diffraction

Native cellulose is the main constituent of natural fibres. Cellulose consists of an alternation of amorphous and crystalline regions. As it is the only element to crystallize in natural fibres it is possible to evaluate the crystallinity rate in such fibre by doing X-Ray diffraction analysis.

X-ray diffractograms were recorded on a Seifert 3003 PTS diffractometer using Cu K α radiation ($\lambda = 1.504018\text{ \AA}$). The diffractometer was used in the symmetrical transmission mode and the intensity was measured as a function of the scattering angle 2θ by θ - 2θ scan. Analysis was realized in 2θ from 10° until 60° with a step of 0.15° and a delay time of 5 s. Spectral analysis was done in the longitudinal and transversal side. For illustration, flax bundle sample used is depicted on **Figure 2**. By using empirical method based on Segal et al. works [30], we calculated the crystallinity degree of the four fibres. Among the different methods developed to determine crystallinity index by X-ray analysis and compared in Thygesen et al. works [31], Segal's method is the simplest, fastest and more frequently used method. Results give qualitative or semi-quantitative information. In practice, sample crystallinity, X_{cr} , is determined by **Equation 1 (Figure 3)** using the height of the (002) peak (I_{002} , $2\theta=22.6^\circ$) and the minimum between the (002) and 110 peaks (I_{AM} , $2\theta=18^\circ$) (**Figure 3**). I_{002} represents both the contribution from crystalline and amorphous material while I_{AM} represents amorphous material only.

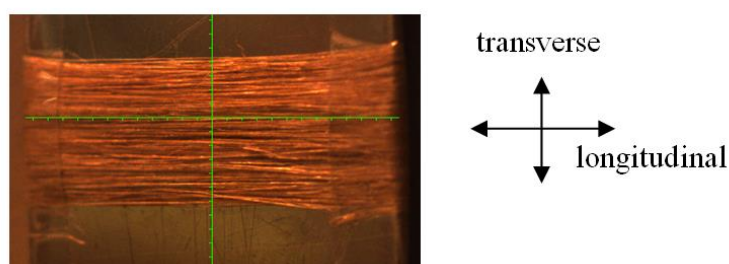


Fig.2 Flax sample used for X-Ray analysis

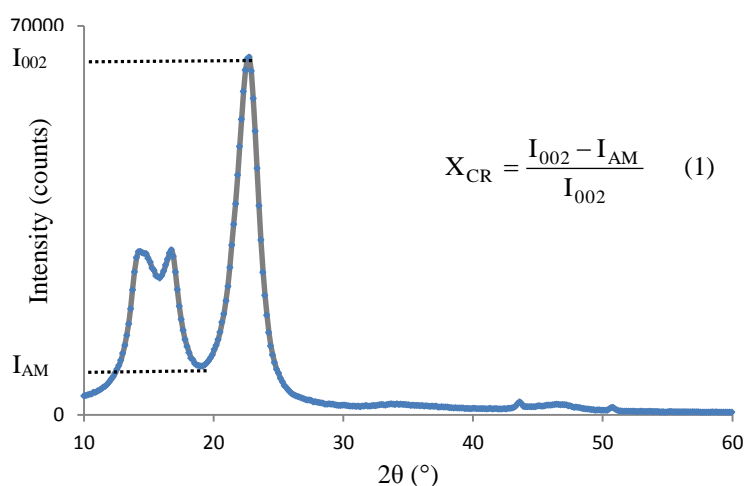


Fig. 3 Segal method

2.2.3. Scanning Electron Microscopy

The fibres morphologies were investigated by Scanning Electron Microscopy using an environmental microscope EVO40 EP from CARL ZEISS Company.

2.2.4. Pycnometry

Densities of the four dried fibres were determined using the classical liquid pycnometry method [33].

2.2.5. Specimen ageing

To study the diffusive behaviour of the four fibres, bundles were submitted to hygro-thermal ageing either in total water immersion at room temperature and in an environmental chamber at 80 % relative humidity and 23°C. Absorption or desorption kinetics has been plotted by doing periodic gravimetric measurements.

In the case of immersion experiments, as it is technically difficult to periodically weigh fibres in liquid water, desorption kinetics has been studied. Thereby, each specimen (**Figure 4**) was first immersed in distilled water at room temperature during 11 days until saturation is reached. Then, they were dried in a desiccators containing silica gel (RH = 7.5 %) kept in room temperature. During drying, the samples were periodically weighed in order to study the weight loss as a function of the time. Data were read to 0.01 mg in a precision balance. The moisture content (M_w) is calculated at several times and is expressed in terms of mass percentage as follows in order to obtain time-dependent desorption curves for each fibre:

$$M_w(\%) = \frac{M(t) - M_0}{M_0} \times 100 \quad (2)$$

where M_0 is the initial weight of the bulk specimens before immersion (ambient conditions) and $M(t)$ is the weight of the specimen at time t .

In the case of relative humidity ageing, specimens were kept in a climatic chamber with RH = 80 % and T = 23°C. Sorption kinetics has been followed by gravimetry.



Fig.4 Specimens aged in hygrothermal environments (a) sisal, (b) jute, (c) flax, (d) hemp

3 Results and discussion

3.1. Characterization

3.1.1. FTIR Spectroscopy

The chemical composition of hemp, jute, flax and sisal fibres was analyzed using FTIR-ATR (Fourier Transform InfraRed spectroscopy - Attenuated Total Reflectance). The interesting peaks have been identified on **Figure 5**. They are summarized in **Table 2** through literature [34-38]. The four fibres have a similar chemical footprint. Absorption bands characteristics of lignin, cellulose and hemicelluloses have been identified (**Table 2**).

The broad absorption band between 3600 cm^{-1} and 3100 cm^{-1} is the characteristic of the O-H stretching vibration and hydrogen bond of the hydroxyl groups assigned by deconvolution to intramolecular or intermolecular hydrogen bonding and free OH hydroxyl [37]. This unstructured absorption band is indirectly linked by water content. Indeed, in a recent work, Olsson and Salmèn [39], studied the effect of water on the FTIR spectra of paper. They showed two peaks in the OH-valency region directly affected by water (at 3600 cm^{-1} and 3200 cm^{-1}). They supposed that the peak observed at 3200 cm^{-1} could be associated with strongly bound water (water bound directly by hydrogen bonds to the OH groups of cellulose and the hemicelluloses) and the peak at 3600 cm^{-1} is associated with more loosely bound water, that is, water indirectly bonded to the OH groups via another water molecule.

The absorption band at 1635 cm^{-1} is assigned by several authors to be characteristic of adsorbed water [35, 37]. This peak testifies the presence of water in the samples. Indeed, in ambient conditions natural fibres contain residual water.

Actually, the principal information, given by the experiment is, first the similarity between each fibres and secondly the spectral footprint of the fibres testifying the presence of hydroxyl and carboxyl functions which lead to moisture absorption in such fibres [40,41].

The Total Crystallinity Index from Nelson and O'Connor's method has been calculated. They are presented in the **Table 3**. The group absorption bands in the 1400-1200 cm^{-1} region are related to the crystalline phase of cellulose. In this range, the one at 1375 cm^{-1} (C-H bending) was chosen as being most suitable for indicating crystallinity [30]......

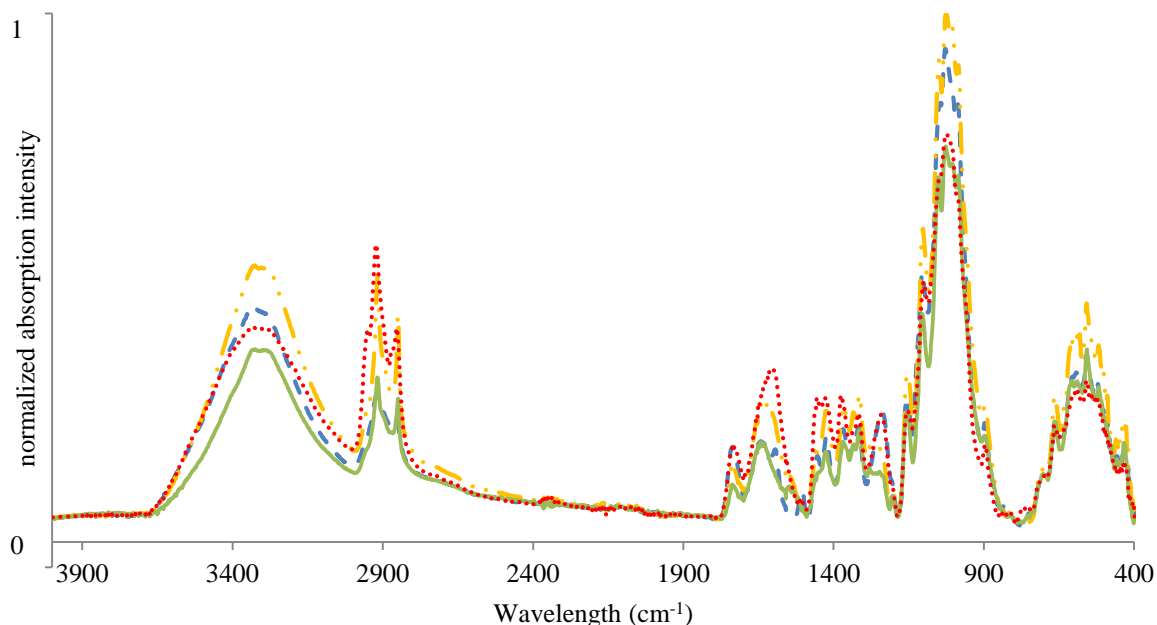


Fig.5 FTIR spectrum of ••• sisal, - - - jute, - · - · flax, — hemp fibres

Wavelength (cm-1)	Assignment
3600-3100	Hydrogen bonded of OH stretching in cellulose, hemicelluloses
2935	CH stretching of cellulose and hemicellulose
2862	CH ₂ stretching of cellulose and hemicellulose
1735	C=O stretching vibration of carboxylic acid in lignin, pectin, wax or ester group in hemicelluloses
1635	Adsorbed water
1595	Aromatic ring in lignin (exclusively jute spectrum)
1502	Aromatic ring in lignin
1425	Carboxylic acid of lignin, pectin or some wax and COO-vibration
1375	CH bending of cellulose and hemicellulose
1335	OH in plane deformation
1315	CH ₂ wagging of cellulose and hemicellulose
1275	lignin
1240	C-O of acetyl in lignin
1160	anti-symmetrical deformation of the C-O-C band
1125-895	C-O stretching and ring vibrational modes
895	Characteristic of β -links in cellulose
700-650	OH out of plane bending

Table 2. Assignment of the main absorption bands in FTIR spectra of sisal, jute, flax and hemp fibres [34-38]

3.1.2. X-ray scattering

In the X-ray diffractograms, presented in **Figure 6**, three peaks were observed for all samples. They are characteristic of the native cellulose crystalline structure I_{β} [42]. The peak at $2\theta = 14.9^\circ$ corresponds to the (110) crystallographic plane, the other one at $2\theta = 16.5^\circ$ corresponds to $(\bar{1}\bar{1}\bar{1})$ plane and the peak at $2\theta = 22.6^\circ$ corresponds to the (002) reflection.

The crystallinity indices were obtained from X-ray diffractograms according to the method based on the intensity measured at two points in the diffractogram, proposed by Segal et al. [31]. They were calculated in both the longitudinal ($\Psi = 0^\circ$) and transverse ($\Psi = 90^\circ$) directions. Results are displayed in **Table 4**.

The X-ray results show two groups of fibres. Hemp and flax fibres have a main crystallinity index of 88 % higher than those of the two other fibres. They are about 10% superior to jute crystallinity index in both directions and about 30% and 15% superior to sisal crystallinity index in longitudinal and transversal direction respectively. Results obtained for a given fibre are almost the same in longitudinal or transversal direction except for sisal. Indeed, in the longitudinal direction, crystallinity index calculated for sisal fibers has to be considered with critical mind. Compared to other fibres, sisal was difficult to handle and a defect in the sample flatness could lead to an incorrect measurement.

Results obtained are overestimated because of some weakness in the method as reported by some authors [43]. Actually, cellulose content in such fibres is reported to be 78% in flax for example [44]. As a consequence, the method gave us only semi-quantitative information to compare the four fibres together. According Nakamura et al. [45], diffusion coefficient inside cellulosic materials have a strong relationship with the amorphous fraction of cellulose, since the water molecule can diffuse only through the amorphous part of cellulose samples. Thereby, moisture absorption should be more important in sisal or jute than in the two others fibres. This hypothesis will be checked later with the analysis of ageing test performed on such fibres (see paragraph 3.2.4).

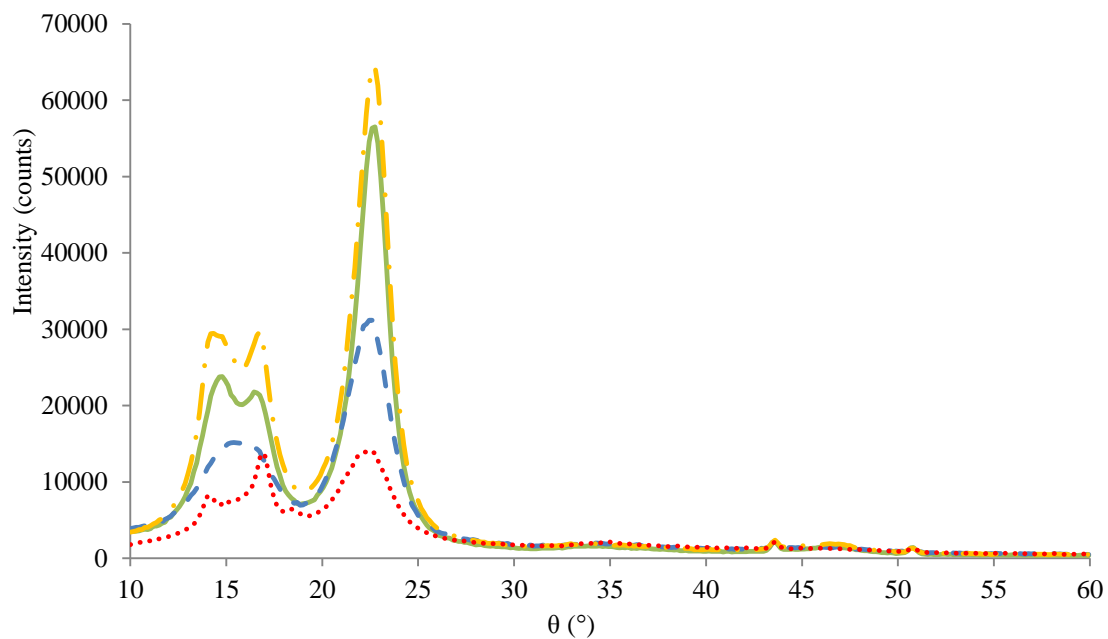


Fig.6 X-ray diffractograms of the four fibres (••• sisal, - - - jute, - . - . flax, — hemp)

	$\Psi = 0^\circ$	$\Psi = 90^\circ$
Sisal	58 %	73 %
Jute	78.4 %	79.9 %

Flax	87 %	88 %
Hemp	88.1 %	88.2 %

Table 4. Crystallinity indices of the fibres in longitudinal $\Psi = 0^\circ$ and transversal $\Psi = 90^\circ$ direction

3.1.3. SEM analysis

SEM observations of the longitudinal surface of the four kinds of fibres were realized. Pictures of jute, sisal, flax and hemp fibres are presented in different scales on **Figure 7 (a), (b) (c) and (d)** respectively. They show the complex structure of natural fibres. It consists of several elementary fibres linked together by the middle lamella composed by pectin that give strength to the bundle. In this area, moisture sorption is enhanced. On **Figure 7 (c)**, the hydrophilic lamella is pointed by the arrow.

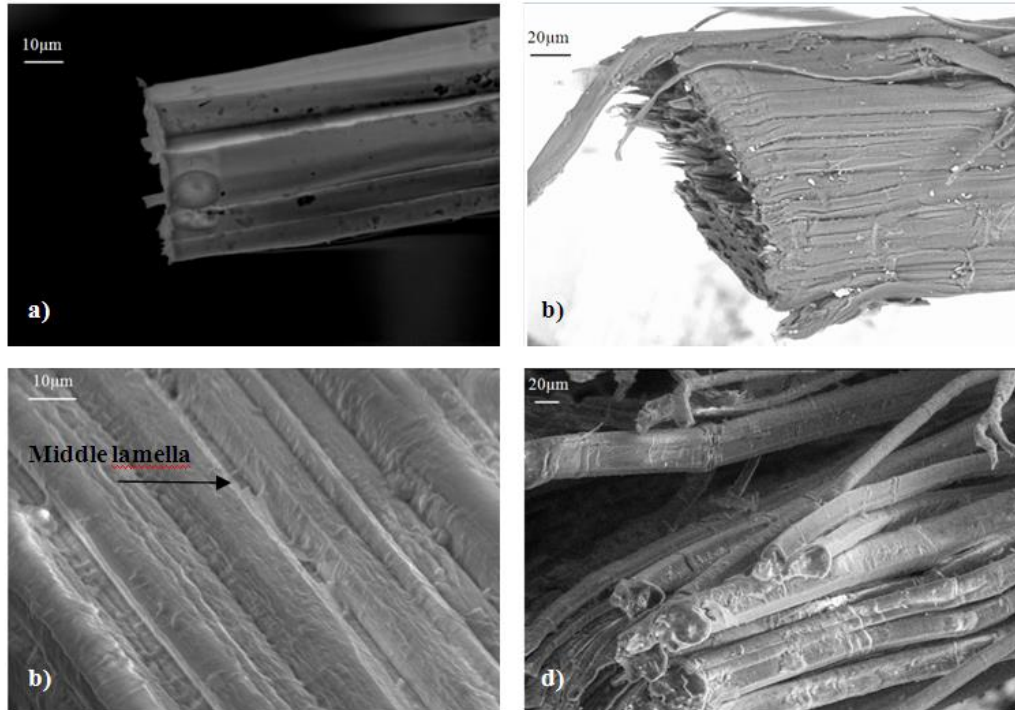


Fig.7 SEM pictures of a) Jute, b) Sisal c) Flax and d) Hemp bundles

3.1.4. Pycnometry

Results deduced from pycnometry tests are presented in **Table 5**. The densities obtained for dried sisal, jute, flax and hemp at room temperature were $1058.2 (\pm 80.8)$, $1201.8 (\pm 55.4)$, $1402.9 (\pm 84.8)$ and $1358.9 (\pm 20.6)$ kg/m^3 , respectively. The density is in the same order for all fibres. These values are consistent to other natural fibres like palm (1030 kg/m^3) and coconut (1150 kg/m^3) and same fibres investigated by others authors [4,23]. All vegetal fibres present densities much lower than glass fibres (2500 kg/m^3). As a consequence, they have interesting specific mechanical properties to compete with glass fibres as presented in Table 1.

The densities deduced from pycnometry analysis are necessary to calculate the water concentration in fibres from the time-dependent mass uptake collected during ageing tests (see section 3.2.4).

Fibre	Density (kg/m^3)
Sisal	1058.2 ± 80.8
Jute	1201.8 ± 55.4
Flax	1358.9 ± 20.6
Hemp	1402.9 ± 84.8

Table 5: Densities of the four studied fibres determined through pycnometry.

3.2. Kinetic's diffusion model

Classical diffusion models used to predict diffusion phenomenon inside polymers (Fick's law, dual stage Fick's law and Langmuir model) have been used for interpreting our experimental results.

3.2.1. Fick's law

The traditional Fickian diffusion model [46] used to predict transport phenomena in numerous environments is the most common model used for predicting the diffusion of moisture in polymeric resins. Besides, the model is consistent with the so-called free volume theory [47].

For the purpose of modeling, fibres have been assumed to be assimilated as a full homogenous cylinder the radius r of which is very small compared to its length. In the case when a long circular cylinder is considered, in which diffusion is radial (one dimensional case), the moisture concentration C is then a function of radius r and time t , only. The corresponding diffusion equation writes as follows [48]:

$$\frac{\partial C}{\partial t} = D \left(\frac{1}{r} \frac{\partial C}{\partial r} + \frac{\partial^2 C}{\partial r^2} \right) \quad (3)$$

where D is the diffusion coefficient.

Indeed, the integration of the analytical solution of Eq. (2), over the cylinder of radius $r = a$ yields the following expression for the moisture uptake:

$$\frac{M_t}{M_\infty} = 1 - \sum_{n=1}^{\infty} \frac{4}{a^2 \alpha_n^2} \exp(-D \alpha_n^2 t) \quad (4)$$

where α_n are the roots of the first species of Bessel's function at order 0, M_t is the moisture content at time t and M_∞ is the moisture content at infinite time.

By minimizing the agreement between the experimental results and the moisture uptake predicted owing to Eq. (3), we determined both the Fickian diffusion coefficients and the saturation mass uptake (M_∞) for each investigated fibre.

3.2.2. Dual stage Fick's law

The dual stage moisture transport model has also been successfully used for predicting and interpreting ageing test, as shown, for instance, in [20]. In the case of an anomalous moisture uptake, Loh et al. developed a dual stage uptake model consisting of two Fickian diffusion kinetics occurring in parallel. Both the Fickian diffusion models use Eq. (4) with separate diffusion coefficient (D_1 and D_2) and saturation levels ($M_{\infty 1}$ and $M_{\infty 2}$), respectively. The sum of each saturation level gives the total moisture absorption capacity of the specimen in the steady state of the diffusion process.

$$M_t = M_{\infty 1} \left(1 - \sum_{n=1}^{\infty} \frac{4}{a^2 \alpha_n^2} \exp(-D_1 \alpha_n^2 t) \right) + M_{\infty 2} \left(1 - \sum_{n=1}^{\infty} \frac{4}{a^2 \alpha_n^2} \exp(-D_2 \alpha_n^2 t) \right) \quad (5)$$

$$M_{\infty 1} + M_{\infty 2} = M_\infty \quad (6)$$

3.2.3. Langmuir law or two-phase model of Carter and Kibler

This model was developed 35 years ago by Carter and Kibler [49]. It is based on the Langmuir theory of adsorption on surface. In this model, the moisture absorption can be explained quantitatively by assuming that absorbed moisture consists of both mobile and bound phases. Molecules of the mobile phase diffuse with a concentration and stress independent diffusion coefficient D_m , and are absorbed (become bound) with a probability per unit time

γ at certain sites (for example: voids within the polymer, hydrogen bonding and heterogeneous morphology). Molecules are emitted from the bound phase, thereby becoming mobile, with a probability per unit time β .

For the one-dimensional case, in a homogeneous cylinder of diameter r , the molecular number densities at time t satisfy the following coupled set of equations:

$$\begin{cases} \frac{\partial n}{\partial t} = D\left(\frac{\partial^2 n}{\partial r^2} + \frac{1}{r} \frac{\partial n}{\partial r}\right) + \frac{\partial N}{\partial t} & (6) \\ \frac{\partial N}{\partial t} = \gamma n - \beta N & (7) \\ \gamma n^\infty = \beta N^\infty & (8) \end{cases}$$

where n is the number of mobile molecules per unit volume and N is the number of bound molecules per unit volume.

These coupled equations are numerically solved by finite difference. We tested different values of the three parameters D , γ , n and β . The triplet which minimizes the square differences between experimental and theoretical results constitutes the best parameters.

3.2.4. Experimental results in immersion

The desorption kinetics (after immersion) of the four fibres are represented on **Figure 8**. On **Figure 8**, the mass at $t = 0$, corresponds to the relative mass gain reaches after 11 days of immersion (M_s). M_s is calculated with **Equation 2** (section 2.2.5), using M_0 as the initial mass before immersion. Then, the relative mass loss against root square time is plotted. Results obtained for the moisture content are displayed on **Figure 8 (a)** whereas water concentration is depicted on **Figure 8 (b)**. Water concentration is deduced from moisture content and the densities measured by pycnometry (section 3.1.4.).

After immersion, the relative mass gain reaches 130 % for sisal, 149 % for hemp, 141 % for flax and 153 % for jute in 11 days. This value could be compared to the works of Bessadok et al. [12]. The authors found a mass gain of 140 % for Alfa fibres in immersion. All fibres have a similar diffusive behaviour. Indeed, characterization achieved previously on the four fibres did show strong similarities of their chemical footprint (IR spectroscopy) as well as their microstructure (SEM). X-ray analysis performed, has shown differences in the crystallinity indices due to difference in cellulose content. In the ageing tests performed here, the correlation between crystallinity degree and water uptake in cellulosic materials supposed by Nakamura et al. [45], is not clear. In bundles of fibres, which contain pore and voids the free water could penetrate inside and could be trapped, which can explain the similarity of the equilibrium water content for the four fibres despite some different crystallinity index

The curves displayed on **Figure 8** have a sigmoid shape that can be the result of a delay time in the establishment of water concentration equilibrium at the fibre surface. After total drying of the sample, the initial weight is not reached (**Figure 8a**). There is a relative mass loss of about 10 % compared to the initial weight for flax, hemp and sisal. Such mass loss could be attributed to the existence of water content in fibres at the initial stage, corresponding to the ambient relative humidity. Drying of other fibres samples in desiccators at room temperature (**Figure 9**) shows a relative mass loss of about 6 %. This initial water is underlined on the FTIR spectra (section 3.1.1.). With jute, the dried fibre mass (after total desorption) is 20 % lower than the initial weight. In this case, in order to rule out the hypothesis of damages in jute fibre, 3 cycles of absorption/desorption was realized. Jute fibres kinetics for the three cycles are presented on the **Figure 10**, only in desorption. Curves do not present any damage. After drying, they always recover the same weight. However, the saturation mass is not exactly the same for all cycles. This could be explained by the man made drying after sample was thrown of water: that stage of the characterization process is actually rather difficult to reproduce in practice.

The three models described before have been used to fit the experimental results. The best adjustment has been achieved by using a classical least-squares method that minimizes the sum of squared residuals, resulting on the difference between experimental results and the fitted value provided by the model. Parameters obtained by identification for each model and each fibre are listed in **Table 6**. The predictive curves are presented on **Figure 11**, where the full line stands for the Fickian model, whereas the dashed line corresponds to Langmuir-type model (predictive curves for dual stage Fickian model are not presented here because the shape was found very close to Fickian results). In order to achieve the numerical simulations according to the predictive models, some changes

in the graphical representation of the results has been done. First, initial mass M_0 has been taken as the saturated fibre mass and secondly, desorption curves have been commuted in absorption kinetics assuming the hypothesis that absorption and desorption behaviour in such fibres is similar. The corresponding representation of the experimental results is depicted on the **Figure 11** through the diamonds curves.

The results show that the classical Fickian diffusion model with a single, constant, diffusion coefficient fails to properly reproduce the experimental uptake curves in all cases. On the opposite, the model originally developed by Carter and Kibler describes very well the kinetics of water uptake in these natural fibres in condition of immersion. Similar diffusion coefficients $D\gamma$ were found for the four fibres. In condition of immersion, there is no data available in literature to be compared with our results. Diffusion coefficient for sisal is almost two times higher than the others. This could be linked to the much important amorphous part inside sisal that makes easier the diffusion. The β coefficient that is the probability of a bound water molecule to become mobile is also higher for sisal. Saturation moisture contents are comparable, in the light of the weak reproducibility of the measurement. The two phases of water considered in the model could be linked to Hatakayema's works [50] dealing with the different kind of water interacting with cellulosic materials. These different kind of water could be separated in two categories. First, the free water (bulk water and capillarity water) which could constitute the mobile phase in the Carter and Kibler model and the bound water (non freezing and freezing bound water) which could be the bonded phase in the diffusion model. By performing cooling of hydrated cellulose in Differential Scanning Calorimetry (room temperature until 200 K), they could find the amount of bound water and free water inside samples. Thereby, the technique developed in Hatakayema's works, could be an experimental solution to valid our model.

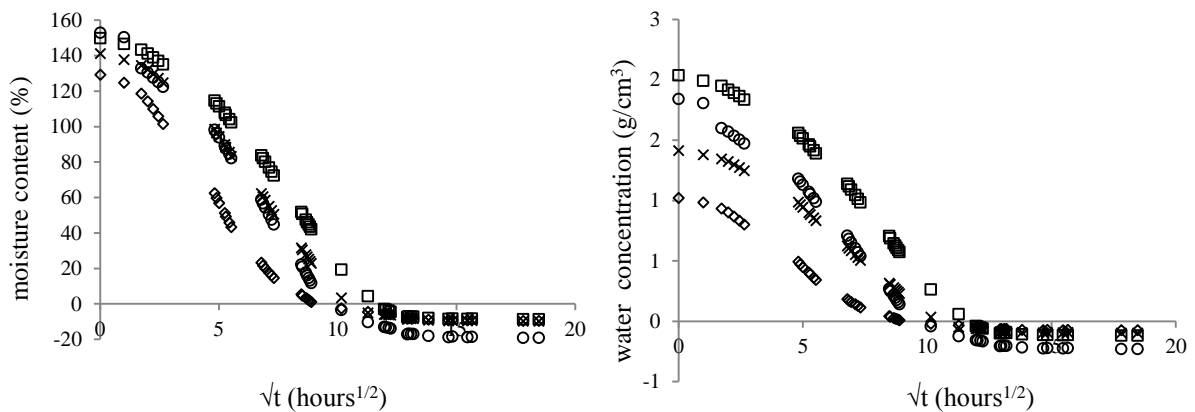


Fig.8 Desorption curves of natural fibres (\diamond sisal, \circ jute, \times flax, \square hemp)

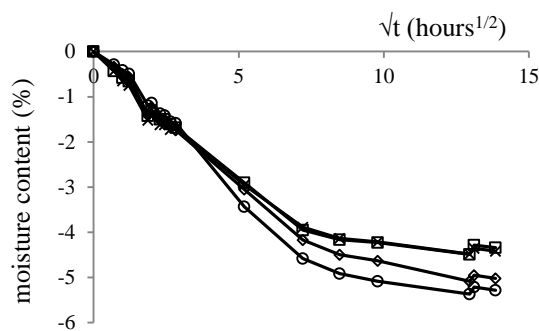


Fig.9 Determination of initial water in fibres (\diamond sisal, \circ jute, \times flax, \square hemp)

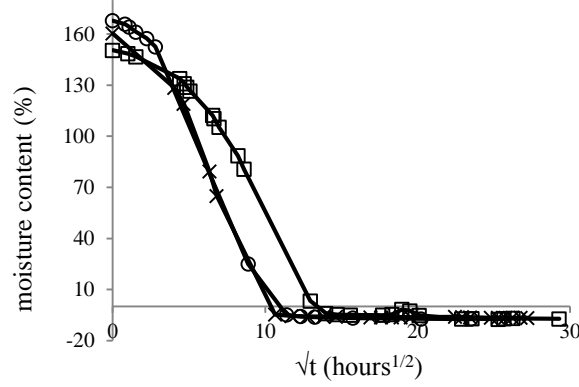


Fig.10 Cycling results for jute fibre bundles (\square 1st cycle, \times 2nd cycle, \circ 3rd cycle)

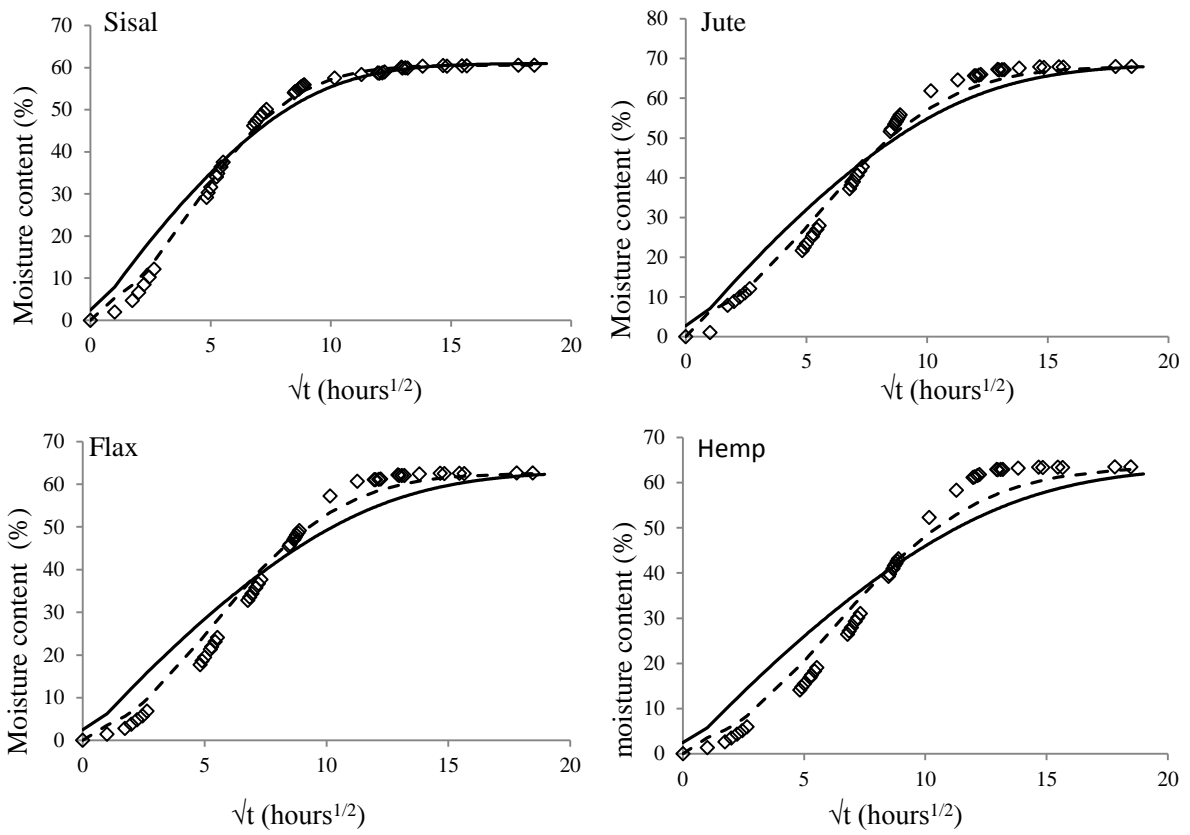


Fig.11 Results for diffusion in immersion (\diamond experimental results, --- Langmuir's model, — Fick's model)

MODEL	PARAMETER	SISAL	JUTE	FLAX	HEMP
FICK	D (mm ² /s)	2.14 10 ⁻⁶	1.12 10 ⁻⁶	1.19 10 ⁻⁶	4.00 10 ⁻⁶
	D ₁ (mm ² /s)	4.00 10 ⁻⁶	2.33 10 ⁻⁶	2.11 10 ⁻⁶	5.29 10 ⁻⁶
DUAL STAGE FICK	D ₂ (mm ² /s)	4.38 10 ⁷	2.30 10 ⁻⁷	2.11 10 ⁻⁷	5.80 10 ⁻⁷
	D _γ (mm ² /s)	9.1 10 ⁻⁶	5.9 10 ⁻⁶	6.8 10 ⁻⁶	5.6 10 ⁻⁶
LANGMUIR	β (s ⁻¹)	8.25 10 ⁻⁶	4.95 10 ⁻⁶	5.75 10 ⁻⁶	4.25 10 ⁻⁶
	M _∞ (%)	60.6	67.8	62.5	63

Table 6. Diffusion parameters determined according to each model.

3.2.5. Experimental results in relative humidity (RH = 80 %)

Absorption kinetics for fibres aged in an environmental chamber with a relative humidity of 80 % are presented on **Figure 12**. The curves are typical of a Fickian diffusion. The corresponding diffusion parameters have been calculated by using Eq. (3). They are presented in **Table 7**. In previously published works, Mannan et al. [13] found a diffusion coefficient of $3.38 \cdot 10^{-7} \text{ mm}^2 \cdot \text{s}^{-1}$ for jute fibres in condition of 51 % relative humidity. As for immersion conditions, all the fibres have similar diffusion parameters.

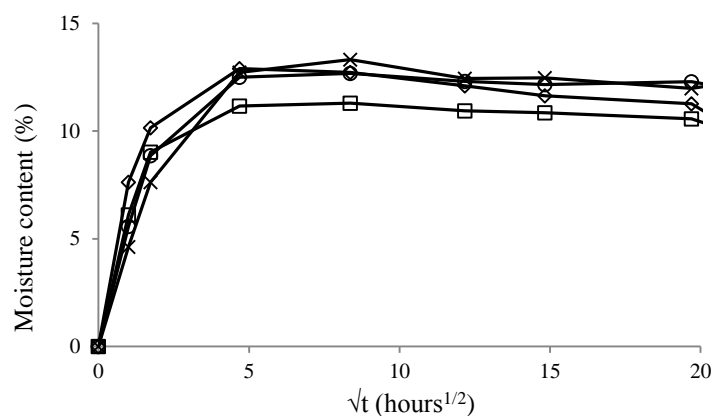


Fig.12 Absorption kinetics of natural fibres in hygrothermal conditions: RH = 80 %, T = 23°C (\diamond sisal, \circ jute, \times flax, \square hemp,)

	SISAL	JUTE	FLAX	HEMP
M_{∞} (%)	11.2	12.3	12.0	10.5
D (mm^2/s)	$1.17 \cdot 10^{-4}$	$4.02 \cdot 10^{-4}$	$2.00 \cdot 10^{-4}$	$2.27 \cdot 10^{-4}$

Table 7. Fickian parameters for fibres aged in hygro-thermal conditions RH = 80 %, T = 23°C

4 Conclusions

First a characterization of four natural fibres has been achieved by using different technical analysis. The characterization enabled us to identify the composition of fibres, estimate the crystallinity degree and observe the complex structure of fibres. Despite their different origins, the four fibres have a similar structure. Then, they have a similar diffusive behaviour.

By performing ageing test we have also shown that natural fibres exposed to moisture in immersion or vapor humidity conditions don't exhibit the same diffusive behaviour. Langmuir theory actually describes very well diffusion inside fibres immersed in liquid water whereas the same fibres follow a Fickian diffusion in the case when they are exposed to vapor during relative humidity ageing. The mass gain in immersion is widely more important than in an environment at 80 % relative humidity. This gap can be explained by the specimen's geometry. Free volume in such fibres is important and liquid water could be trapped inside pores. In vapor conditions it is possible that some water molecules remain in a gaseous state within the void parts of the samples. Since gaseous water could be released easily, the mass gain is less important. In both case there is no damage according to the absorption and desorption cycles.

In the case of immersion, the observed curvature of the time dependent weight-gain could be attributed to effects induced by mechanical states on the diffusion of moisture. Upcoming investigations will be focused on the use of more advanced multi-physics theoretical approaches dedicated to the modeling of the moisture uptake occurring while the heterogeneous, local swelling experienced by the polymer is accounted for. Such a model, recently published in the literature by Sar et al. [51], should provide a more realistic framework for interpreting the ageing tests achieved on natural fibres, in particular in the cases when immersion conditions are considered.

Acknowledgments

The authors would like to acknowledge Dr Annick Perronnet for its help and its experience during SEM sessions.

References

1. Summerscales, J.; Dissanayake, N.; Hall, W. and Virk, A.S. *Composite Part A*. **2010**, *41*, 1329-1335.
2. Wambua, P., Ivens, J. and Verpoest, I. *Compos. Sci. Technol.* **2003**, *63*, 1259–1264.

3. Suddell, B.C.; Evans, W.J. In: *Biopolymers & Their BioComposites*; Mohanty, A.K.; Misra, M. Drzal, L.T., Eds; CRC Press, **2005** pp. 231-259.
4. Bledzki, A.K. and Gassan, J. *Prog. Polym. Sci.* **1999**, *24*, 221–274.
5. Stamboulis, A.; Baillie, C.A. and Peijs, T. *Composites Part A.* **2001**, *32*, 1105-1115.
6. Lee, J.M.; Pawlak, J.J. and Heitmann, J.A. *Mater. Charact.* **2010**, *61*, 507-517.
7. Rangaraj, S.V. and Smith, L. *J. Thermoplast. Compos. Mater.* **2000**, *13*, 140-61.
8. Costa, F.H.H.M. and D'almeida, J.R.M. *Polym-Plast. Technol.* **1999**, *38*, 1081-94.
9. Mishra, S.; Naik, J. and Patil Y. *Compos. Sci. Technol.* **2000**, *60*, 1729–35.
10. Hill, C.A.S.; Abdul Khalil, H.P.S. and Hale, M.D. *Ind. Crop. Prod.* **1998**, *8*, 53-63.
11. Alix, S., Lebrun, L., Morvan, C. and Marais, S. *Compos. Sci. Technol.* **2011**, *71*, 893–899.
12. Bessadok, A., Marais, S., Gouanvé, F., Colasse, L., Zimmerlin, I., Roudesli, S. and Metayer, M. *Compos. Sci. Technol.* **2007**, *67*, 685-697.
13. Mannan, Kh.M. and Talukder M.A.I. *Polymer* **1997**, *38*, 2493-2500.
14. Gouanve, F., Marais, S., Bessadok, A., Langevin, D. and Metayer M. *Eur. Polym. J.* **2007**, *43*, 586–598.
15. Jedidi, J., Jacquemin, F. and Vautrin, A. *Composites Part A.* **2006**, *37*, 636–645.
16. Autran, M., Pauliard, R., Gautier, L., Mortaigne, B., Mazeas F. and Davies P. *J. Appl. Polym. Sci.* **2002**, *84*, 2185–2195.
17. Zhou, J. and Lucas J.P. *Polymer* **1999a**, *40*, 5505-5512.
18. Roy, S., Xu, W.X.; Park S.J. and Liechti K.M. *J. Appl. Mech.* **2000**, *67*, 391-397.
19. Popineau, S., Rondeau-Mouro, C., Sulpice-Gaillet, C. and Shanahan M.E.R. *Polymer* **2006**, *46*, 10733–10740.
20. Loh, W.K.; Crocombe, A.D.; Abdel Wahab, M.M. and Ashcroft I.A. *Int. J. Adhes. Adhes.* **2005**, *25*, 1–12.
21. Kohler, R.; Dück, R.; Ausperger, B. and Alex R. *Compos. Interfaces.* **2003**, *10*, 255-276.
22. Jacquemin, F.; Fréour, S. and Guillén R. *Compos. Sci. Technol.* **2006**, *66*, 397–406.
23. Satyanarayana, K.G. and Wipych, F. In: *Engineering biopolymers: Homopolymers, Blends and Composites*. Fakirov, S., Bhattacharyya, D., Eds; Munich: Hanser Publishers, **2007**. pp. 3-48.
24. Oksman, K.; Skrifvars, M.; Selin, J.F. *Compos. Sci. Technol.* **2003**, *63*, 1317–1324.
25. Morvan, C.; Andème-Onzighi, C.; Girault, R.; Himmelsbach, D.S.; Driouich, A. and Akin, D.E. *Plant Physiol. Biochem.* **2003**, *41*, 935-944.
26. Gorshkova, T.; Gurjanov, O.; Mikshina, P.; Ibragimova, N.; Mokshina, N.; Salnikov, V.; Ageeva, M.V., Amenitskii, S.I., Chernova, T.E. and Chemikosova, S.B., *Russ J Plant Physiol+*. **2010**, *57*, 328-341.
27. Hearle, J.W.S. *J. Appl. Polym. Sci.* **1963**, *7*, 1207-1223.
28. Baley, C. *Composites Part A.* **2002**, *33*, 939-948.
29. Siroky, J.; Blackburn, R.S.; Bechtold, T.; Taylor, J.; White, P. *Cellulose.* **2010**, *17*, 103–115.
30. Nelson, M.L.; O'Connor, R.T. *J. Appl. Polym. Sci.* **1964b**, *8*, 1325–1341.

31. Segal, L.; Creely, J.J.; Martin, A.E. and Conrad, C.M. *Text. Res. J.* **1959**, *29*, 786–794.
32. Thygesen, A.; Oddershede, J.; Lilholt, H.; Thomsen, A.B.; Stahl K. *Cellulose.* **2005**, *12*, 563-576.
33. Pratten, N.A. *J. Mater. Sci.* **1981**, *16*, 1737-1747.
34. Liang, C.Y.; Marchessault, R.H. *J. polym. Sci.* **1959**, *39*, 269-278.
35. Marchessault, R.H. *Pure Appl. Chem.* **1962**, *5*, 107-130
36. Nelsson, M.L.; O’Connor, R.T. *J.Appl. Polym. Sci.* **1964a**, *8*, 1311-1324.
37. Kondo, T. *Cellulose*, 1997, *4*, 281-292.
38. De Rosa, I.M.; Kenny, J.M.; Puglia, D., Santulli, C. and Sarasini, F. *Compos. Sci. Technol.* **2010**, *70*, 116-122.
39. Olson, A.M. and Salmen, L. *Carbohydr. Res.* **2004**, *339*, 813-818.
40. Davies, G.C. and Bruce, D.M. *Text. Res. J.* **1998**, *60*, 623-629.
41. Cousins, W.J. *Wood Sci. Technol.* **1978**, *12*, 1319-1228.
42. Sarko, A. and Muggli, R. *Macromolecules* **1974**, *7*, 486–494.
43. Park, S.; Baker, J.O.; Himmel, M.E.; Parilla, P.A. and Johnson, D.K. *Biotechnol Biofuels*, **2010**, *3*:10.
44. Le Duigou, A. Contribution à l’étude des biocomposites. Ph.D. Thesis, Université de Bretagne Sud, **2010**.
45. Nakamura, K.; Hatakeyama, T.; Hatakeyama, H. *Text. Res. J.* **1981**, *51*, 607-613.
46. Fick A. Ueber Diffusion. *Annalen der Physik* **1855**; *170*:59–86 .
47. Eyring, H. Viscosity. *J. Chem. Phys.* **1936**, *4*, 283-291.
48. Crank, J. *The mathematics of diffusion.* Clarendon Press, Oxford, **1975**.
49. Carter, H. and Kibler, K. *J. Compos. Mater.* **1978**, *12*, 118-131.
50. Hatakeyama, H.; Hatakeyama, T. *Thermochim. Acta.* 1998, *308*, 3-22.
51. Sar, B.E.; Fréour, S.; Davies, P. and Jacquemin, F. *Eur. J. Mech.* **2012**, *36*, 38-43.

Figures Captions

Fig.1 Multi-scale structure of the flax fibre [23,26]

Fig.2 Flax sample used for X-Ray analysis

Fig.3 Specimens aged in hygrothermal environments (a) sisal, (b) jute, (c) flax, (d) hemp

Fig.4 FTIR spectrum of – sisal, - - jute, - - flax and - - hemp fibres

Fig.5 X-ray diffractograms of the four fibres (⋯ sisal, --- jute, —⋯ flax, — hemp)

Fig.6 SEM pictures of a) Jute, b) Hemp and c) Flax fibres

Fig.7 Desorption curves of natural fibres (×flax, □hemp, ◇sisal, ○jute)

Fig.8 Determination of initial water in fibres (×flax, □hemp, ◇sisal, ○jute)

Fig.9 Cycling results for hemp jute fibre bundles (□1st cycle, × 2nd cycle, ○3rd cycle)

Fig.10 Results for diffusion in immersion (◇ experimental results, --- Langmuir's model, — Fick's model)

Fig.11 Absorption kinetics of natural fibres in hygrothermal conditions: RH = 80 %, T = 23°C (×flax, □hemp, ◇sisal, ○jute)

Tables Captions

Table 1. Mechanical properties of different fibres [23,24,28].

Table 2. Crystallinity indices of the fibres in longitudinal $\Psi = 0^\circ$ and transversal $\Psi = 90^\circ$ direction.

Table 3: Densities of the four studied fibres determined through pycnometry.

Table 4. Diffusion parameters determined according to each model.

Table 5. Fickian parameters for fibres aged in hygro-thermal conditions RH = 80 %, T = 23°C.